

# Top physics studies at the LHC in the Standard Model and beyond with the ATLAS detector

**Susana Cabrera (on behalf of the ATLAS Collaboration)**

Instituto de Física Corpuscular, IFIC (CSIC – UVEG),  
Edificios de Investigación, Aptdo de Correos 22085, Valencia, E-46071, Spain  
E-mail: [Susana.Cabrera@ific.uv.es](mailto:Susana.Cabrera@ific.uv.es)

**Abstract.** The LHC will be a top quark factory, producing large numbers of top quarks even at the initial low luminosities. This will enable a rich program of top quark physics to be explored, both within the Standard Model and using top quarks as probes of physics beyond the Standard Model. Recent studies from ATLAS are presented, including prospects for the measurements of the production of top pairs and single top production, angular correlations in the top decay, and the precision measurement of the top quark mass. The search for physics beyond the Standard Model will be illustrated with searches for rare top decays involving Flavour Changing Neutral Currents, and the reconstruction of  $t\bar{t}$  resonances resulting from new heavy particles in various models.

## 1. Introduction

The field of top quark physics is currently at a very tantalizing stage. For the time being, real top quarks are produced in the proton-antiproton collisions delivered by the Tevatron collider at center of mass energies of  $\sqrt{s} = 1.96$  TeV during the Run 2. At the end of the year 2008, this collider has delivered an integrated luminosity of  $5.5 \text{ fb}^{-1}$ . The CDF and DØ experiments have collected  $4.5 \text{ fb}^{-1}$  and  $4.7 \text{ fb}^{-1}$  respectively. Some of the top quark physics analyses have considered integrated luminosities up to  $3 \text{ fb}^{-1}$ . Besides the precise measurement of the mass:  $M_{top} = 172.4 \pm 1.2 \text{ GeV}$  [1], with a relative uncertainty of 0.7%, and the measurement of the top pair production cross section,  $\sigma(p\bar{p} \rightarrow t\bar{t}) = 7.02 \pm 0.63 \text{ pb}$  for  $M_{top} = 175 \text{ GeV}$  [2], with a relative uncertainty of 9% that reaches the current accuracy of the NLO QCD calculations, the rest of measurements of top quark properties are still very statistically limited (see the public web sites of the CDF and DØ top physics groups for a detailed summary: [3] and [4] respectively).

The proton-proton Large Hadron Collider (LHC) will be a true top quark factory due to the high production cross section of top quark pairs:  $833 \pm 100 \text{ pb}$  [5], that increases by two orders of magnitude with respect to the one at the Tevatron:  $6.73^{+0.71}_{-0.79} \text{ pb}$  [6],  $6.73^{+0.72}_{-0.63} \text{ pb}$  [7],  $6.90^{+0.46}_{-0.64} \text{ pb}$  [8]. The LHC started operations on Sept. 10th of 2008, establishing circulating beams of protons in both directions. These data have allowed the LHC experiments to gain experience in issues related to detector timing, alignment and calibration and therefore, to improve their readiness towards recording the first colliding data [9]. On Sept 19th an incident happened during the commissioning of the sector 3-4. The understanding of the problem, an electrical failure in the interconnection of two LHC magnets, has been followed by the repair of the damaged elements of the accelerator, and the establishment of prevention measurements

to diagnose and hopefully avoid similar problems in the future operation of the LHC [10]. The latest schedule is to restart operation late in the fall of 2009 [11], with a clear goal for a long first physics run through winter 2009 to autumn 2010 at center of mass energies of  $\sqrt{s} = 10$  TeV. The ATLAS collaboration has recently evaluated the performance of the ATLAS experiment and the prospects for its broad physics program at a center of mass energy of  $\sqrt{s}=14$  TeV [12]. These proceedings are dedicated to review the most relevant issues of the chapter dedicated to top quark physics.

## 2. The production of top quarks in pairs

### 2.1. The semi-leptonic channel: $t\bar{t} \rightarrow W(\rightarrow e/\mu + \nu_{e/\mu})bW(\rightarrow qq')b$

In this channel, a robust technique has been developed to identify  $t\bar{t}$  semi-leptonic events without making use of offline b-tagging algorithms which can determine which jets are likely to have been produced by the hadronisation of b-quarks. The event selection starts with the requirement of a single isolated and high  $p_T$  electron or muon trigger. The subsequent offline selection requires a  $t\bar{t}$  candidate event to have one reconstructed lepton (electron or muon) with transverse momentum  $p_T > 20$  GeV, missing transverse energy  $E_T^{miss} > 20$  GeV, at least four jets with  $p_T > 20$  GeV and among them, at least three jets with  $p_T > 40$  GeV.

After the event selection, the top quark decay candidate is defined using the following experimental hypothesis: the three-jet combination of all jets whose vector sum of four-momenta provides the highest  $p_T$  is originated by the top quark decay chain:  $t \rightarrow bW(\rightarrow qq')$  (see left plot in figure 1). From the previous three-jet combination, the combination of pairs of jets whose vector sum of four-momenta maximizes the transverse momentum is assumed to be originated by a  $W$ -boson hadronic decay  $W(\rightarrow qq')$  and it is used to build the dijet mass distribution of hadronically decaying  $W$  bosons. Additional requirements are applied to increase the purity of the event selection. The  $W$ -boson mass constraint consists of requiring among the three jets, at least one pair with dijet invariant mass within 10 GeV of the peak value of the dijet mass distribution of hadronically decaying  $W$  bosons. In the central plot of figure 1 the large reduction of the  $t\bar{t}$  combinatorial background can be clearly seen. This background consists of  $t\bar{t}$  candidate events with wrong assignments of jets to the quarks from the true hadronic top decay  $t \rightarrow bW(\rightarrow qq')$ . The selection efficiencies for semi-leptonic electron and muon default analyses are: (a) 18.2 % for  $t\bar{t} \rightarrow W(\rightarrow e\nu_e)bW(\rightarrow qq')b$  events and (b) 23.6 % for  $t\bar{t} \rightarrow W(\rightarrow \mu\nu_\mu)bW(\rightarrow qq')b$  events. After the  $W$  mass constraint these efficiencies are reduced down to 9.2 % and 12.0 % respectively. The resulting set of  $t\bar{t}$  event candidates constitutes an excellent sample for commissioning the offline b-tagging algorithms and to determine the light jet energy scale using the decay  $W(\rightarrow qq')$ . Further requirements of one or two b-tagged jets improves the purity of the sample by a factor greater than three. However, the signal efficiency is also reduced by a factor of three (see table 2.1).

The  $t\bar{t}$  cross section is obtained with two methods. The first one, called the counting method, derives the cross section using the ratio:  $\sigma = \frac{N_{obs} - N_{bkg}}{\mathcal{L}\epsilon}$  where  $N_{obs}$  is the total number of events passing the trigger requirements and off-line event selection criteria,  $N_{bkg}$  is the total number of background events,  $\mathcal{L}$  is the integrated luminosity and  $\epsilon$  is the total efficiency, that includes geometrical acceptance, trigger and event selection efficiencies. The method is very sensitive to the uncertainty in the background contribution of the process  $W + \text{jets}$ , estimated from Alpgen  $W + \text{jets}$  Monte Carlo. The Jet Energy Scale (JES) is also a significant systematic error. The advantage of the counting method is that no use is made of the shapes of distributions, that may not be properly described by MC simulations in the commissioning phase of the experiment. A second method uses a maximum likelihood fit of the three-jet mass distribution. The Gaussian signal on top contains completely reconstructed  $t\bar{t}$  events that are truly originated by the top quark decay chain:  $t \rightarrow bW(\rightarrow qq')$  according to information on the matching between quarks and reconstructed jets. The background is described with a Chebychev polynomial and includes combinatorial  $t\bar{t}$  background and background coming from other Standard Model processes (see

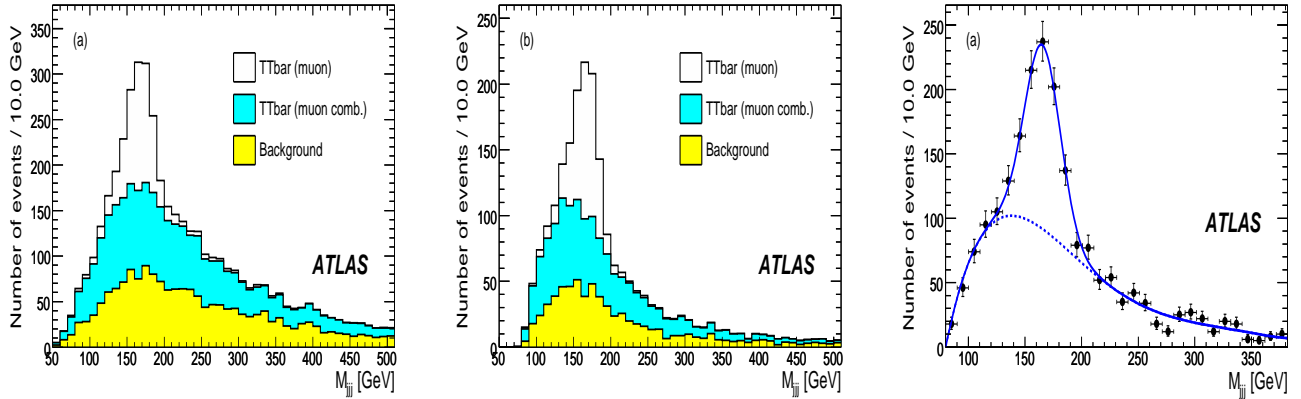


**Figure 1.** Left: Invariant mass of the three-jet combination with highest  $p_T$  for the default event selection. In yellow (light gray) and blue (dark grey), the background contributions from other non  $t\bar{t}$  Standard Model processes and from the  $t\bar{t}$  combinatorial background respectively. Central: after the  $W$  constraint is applied. Right: same as central plot with fit to Gaussian plus Chebychev polynomial functions.

right plot in figure 1). The likelihood fit method is rather insensitive to the total rate of the  $W$ +jets background. The main systematic uncertainty is due to the knowledge of the shape of the fit function.

**Table 1.** Characteristics of the semi-leptonic  $t\bar{t}$  electron and muon samples obtained with  $\mathcal{L} = 100 \text{ pb}^{-1}$  before and after various requirements to increase their purity:  $W$  mass constraint, one and two b-tagged jets. For all cases: expected number of signal events, background composition, total background and signal to background ratio.

$\mathcal{L} = 100 \text{ pb}^{-1}$	$t\bar{t} \rightarrow W(\rightarrow e\nu_e)bW(\rightarrow qq')b$				$t\bar{t} \rightarrow W(\rightarrow \mu\nu_\mu)bW(\rightarrow qq')b$				
	Process	default	$W$ const.	1 b-tag	2 b-tags	Process	default	$W$ const.	1 b-tag
$t\bar{t}$ signal	2555	1262	329	208	3274	1606	403	280	
hadronic $t\bar{t}$	11	4	0.6	0.0	35	17	5	2	
$W$ +jets	761	241	7	1	1052	319	11	0.0	
single top	183	67	18	7	227	99	19	10	
$Z \rightarrow \ell\ell + \text{jets}$	115	35	2	0.4	84	23	0.5	0.0	
$Wb\bar{b}$	44	15	5	0.7	64	19	5	2	
$Wc\bar{c}$	19	6	0.4	0.0	26	9	0.1	0.0	
$WW, WZ, ZZ$	11.5	5.2	0.0	0.0	14.7	6.3	0.0	0.0	
Background	1144	374	33	10	1497	495	42	14	
S/B	2.2	3.4	10.0	20.8	2.2	3.2	9.6	20.1	

## 2.2. Di-lepton channel: $t\bar{t} \rightarrow W(\rightarrow e/\mu\nu_{e/\mu})bW(\rightarrow e/\mu\nu_{e/\mu})b$

The di-lepton  $t\bar{t}$  sample will be collected with single lepton and dilepton triggers with high efficiency. The offline selection requires two oppositely-charged and isolated high  $p_T$  leptons (ee,  $\mu\mu$  and  $e\mu$ ). Three methods have been considered to extract the  $t\bar{t}$  cross section:

- A standard counting method, that uses two additional requirements on the  $E_T^{miss}$  and dilepton invariant mass. In  $100 \text{ pb}^{-1}$ , the optimized selection provides 987  $t\bar{t}$  dilepton events in the three dilepton channels, with an averaged efficiency of 11 %. The main backgrounds are  $Z \rightarrow ee, \mu\mu, \tau\tau$  (57%),  $t\bar{t}$  semi-leptonic (17%),  $W + \text{jets}$  events with jets wrongly identified as electrons or muons, dibosons and single top. The total background is 228 events and the signal to background ratio is better than 4 without b-tagging requirements.
- An inclusive template method, where the two-dimensional distribution of  $E_T^{miss}$  versus  $N_{jets}$  is used to separate di-leptonic  $t\bar{t}$  from background processes WW and  $Z \rightarrow \tau\tau$  and to extract the cross section with a two-dimensional binned likelihood fit of this distribution.
- A likelihood method, that uses a log-likelihood function to extract the number of signal and background events where the signal and background distributions are described with the angular separations between the highest  $p_T$  lepton and the highest  $p_T$  jet with respect to the  $E_T^{miss}$  vector.

For all the three methods, the JES uncertainty is the largest contributor to the systematic uncertainty. In table 2 the experimental precision achieved with all the methods reviewed in semi-leptonic and di-leptonic  $t\bar{t}$  channels are compared. With an integrated luminosity of  $100 \text{ pb}^{-1}$ , all the measurements will be dominated by systematic rather than statistical errors, even in the di-leptonic channel. At the LHC start-up, the expected uncertainty of the luminosity will be 20-30% due to the rough initial measurement of the machine parameters. This uncertainty will be reduced down to 5% due to the use of better techniques and dedicated detectors as well as improving the knowledge of the accelerator parameters.

**Table 2.** Summary of the expected precision of the measurements of the top pair production cross section with different experimental methods developed by the ATLAS collaboration and considering a data sample with an integrated luminosity of  $\mathcal{L} = 100 \text{ pb}^{-1}$  in comparison with the current Tevatron precision [2].

ATLAS $\mathcal{L} = 100 \text{ pb}^{-1}$	$\Delta\sigma/\sigma(\text{stat})$	$\Delta\sigma/\sigma(\text{syst})$	$\Delta\sigma/\sigma(\text{pdf})$	$\Delta\sigma/\sigma(\text{lum})$
Di-lepton channel: counting method	$\pm 4\%$	$\pm 2\%$	$\pm 2\%$	$\pm 20\text{-}30\%$
Di-lepton channel: inclusive method	$\pm 4\%$	$\pm 4\%$	$\pm 2\%$	$\pm 20\text{-}30\%$
Di-lepton channel: likelihood method	$\pm 5\%$	$\pm 8\%$	$\pm 0.2\%$	$\pm 20\text{-}30\%$
Single lepton channel: likelihood method	$\pm 7\%$	$\pm 15\%$	$\pm 3\%$	$\pm 20\text{-}30\%$
Single lepton channel: counting method	$\pm 3\%$	$\pm 16\%$	$\pm 3\%$	$\pm 20\text{-}30\%$
CDF combination $\mathcal{L} = 3 \text{ fb}^{-1}$ : $\pm 9\%$	$\pm 3\%$	$\pm 6\%$		$\pm 3\%$

### 3. Single top production

The  $D\emptyset$  collaboration has presented evidence for production of single top quarks via s-channel and t-channel together:  $p\bar{p} \rightarrow tb + X, tqb + X$  in a data sample of  $\mathcal{L} = 0.9 \text{ fb}^{-1}$  with a 3.4 standard deviation significance [13]. The most sensitive analysis from CDF is based on a neural network technique with  $\mathcal{L} = 2.7 \text{ fb}^{-1}$  and it reaches 3.8 standard deviation significance and 5 standard deviation expected significance [14]. The  $5\sigma$  observation is around the corner [15]. However the measurements with the single top quark sample will be limited by the available data statistics. Due to the increased single top production cross section at the LHC, ATLAS will have higher statistics to study top quark properties and to search for new physics, for instance, charged Higgs,  $W'$  bosons. The most promising channel for single top quark observation at the LHC is the t-channel, with the largest theoretical cross section (see first two rows of table 3). The

associated production  $Wt$ , not considered at the Tevatron due to the tiny cross section, will be the second most promising channel at the LHC.

**Table 3.** Theoretical predictions for single top production cross section at the Tevatron and at the LHC for t-channel, s-channel and associated  $Wt$  production, together with event yields for signal and background processes. Uncertainties in event yields come from Monte Carlo statistics only. For t-channel, sequential cut based and Multivariate BDT analyses are compared. Signal to background ratios and statistical significance are also given. The signal to background is better than one for the t-channel and using the BDT Multivariate technique.

	t-channel		s-channel	Wt production
	$\sigma(p\bar{p}/pp \rightarrow tqb + X)$	$\sigma(p\bar{p}/pp \rightarrow tb + X)$	$\sigma(p\bar{p}/pp \rightarrow Wt)$	
Tevatron	$1.98 \pm 0.25$ pb	$0.88 \pm 0.11$ pb	not considered	
LHC	$246 \pm 12$ pb	$11 \pm 1$ pb	$66 \pm 2$ pb	
Analysis Type	Seq. Cut	BDT	Seq. Cut	Seq. Cut.
Single top signal	$1460 \pm 56$	542	$24.8 \pm 1.3$	$639.0 \pm 19.5$
Other Single top	$148 \pm 9$	18	$39.5 \pm 8.2$	$1417.6 \pm 50.0$
$t\bar{t}$	$2816 \pm 65$	184	$145.1 \pm 12.7$	$3022.0 \pm 58.2$
$W + \text{jets}, W\bar{b}$	$942 \pm 37$	211	$66.4 \pm 3.4$	$3384.0 \pm 80.9$
Total background	$3906 \pm 75$	413	$251.0 \pm 15.5$	$7823.6 \pm 111.5$
$\frac{S}{B}$	37%	1.31	9.8%	8.1%
$\frac{S}{\sqrt{B}}$	23.4	26.6	1.6	7.2

Inclusive isolated electron and muon triggers will be used to collect the single top quark events. A common preselection for the three channels requires one high  $p_T$  and isolated electron or muon, vetoing a second isolated lepton,  $E_T^{\text{miss}} > 20$  GeV, at least two jets with  $p_T > 30$  GeV and  $|\eta| \leq 5.0$  and among them, at least one must be b-tagged and  $|\eta| < 2.5$ . For each channel, additional specific requirements are imposed. In table 3 it can be seen that with analyses based on sequential cuts, the signal to background ratio is always lower than one. For this reason, multivariate analyses have been developed. Nevertheless, the statistical significance is good for t-channel and associated  $Wt$  production.

For the t-channel, the specific extra requirements are:  $p_T > 50$  GeV for the b-tagged jet to reject  $W + \text{jets}$  background and  $|\eta| > 2.5$  for the hardest light jet to reject the  $t\bar{t}$  background. The last cut, very efficient in rejecting  $t\bar{t}$  background, is not very efficient in preserving the single top signal. When extracting  $\sigma(pp \rightarrow tqb + X)$  using a sequential cut-based method, the systematic uncertainty is dominated by the theoretical error in the cross section of background processes. JES and b-tagging efficiency are also large contributors.

A Multivariate analysis technique that uses the Boosted Decision Tree (BDT) method has been developed to reject  $t\bar{t}$  background and consequently, to reduce systematics in the cross section measurement. The  $\eta$  cut for the hardest light jet is removed at this point. The BDT method uses a set of variables less sensitive to the Jet Energy Scale systematic uncertainty, for instance: angular separations between the jets and the leading jet, the leading non-b-tagged jet and the lepton. In figure 2 it can be observed the good level of rejection of the  $t\bar{t}$  background obtained with this technique.

With  $\mathcal{L} = 1 \text{ fb}^{-1}$ , the total uncertainty in the measurement of  $\sigma(pp \rightarrow tqb + X)$  is reduced from 45% with the cut-based analysis down to a 23% level with the BDT analysis. This leads to a precision in the production cross section measurement of  $\Delta\sigma/\sigma = \pm 5.7\%_{\text{stat}} \pm 22\%_{\text{sys}} = \pm 23\%$ .

Then, the precision in the measurement of the CKM matrix element,  $V_{tb}$ , will be of  $\Delta V_{tb}/V_{tb} = \pm 11\%_{stat+syst} \pm 4\%_{theo} = \pm 12\%$ .

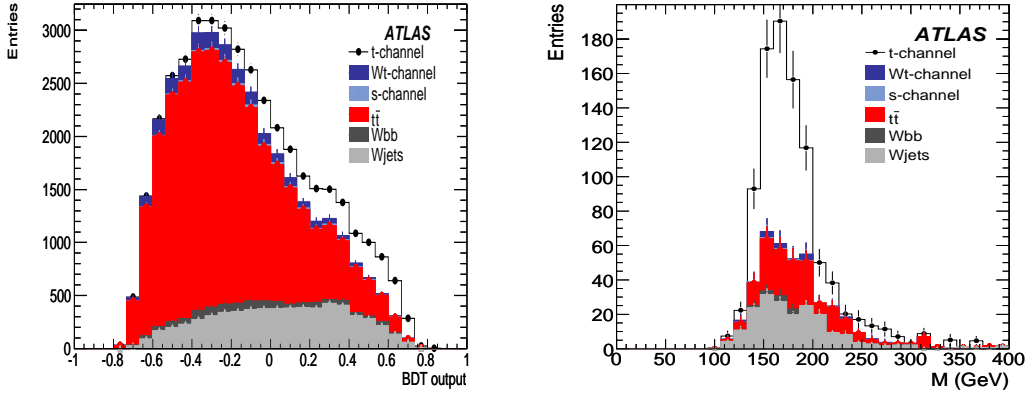


**Figure 2.** Left: BDT output for signal single top t-channel and background. Right: distribution of the leptonic top quark mass using a cut of 0.6 in the BDT output.

#### 4. Top quark mass

A precise measurement of the top quark mass is important since it can be used to constrain the mass of the Higgs boson in the Standard Model. With the aim of determining the top quark mass with high precision, two experimental methods have been developed by the ATLAS collaboration using the semi-leptonic  $t\bar{t}$  sample. In both methods, the best estimator of the top mass is the peak of the invariant mass distribution of the two light-quark jets and the b-quark jet coming from the hadronic top quark decay chain  $t \rightarrow bW(\rightarrow qq')$ . For the top mass measurement, an event selection more stringent than the one described in the previous section 2.1 has been required: at least 4 jets with  $p_T > 40$  GeV and among these jets, exactly two must be b-tagged.

In the first method, the selection of the pair of jets coming from the hadronic  $W$  boson decay is performed via a minimization of the function:

$$\chi^2 = \frac{M_{jj}(\alpha_{E_{j1}}, \alpha_{E_{j2}}) - M_W^{PDG}}{(\Gamma_W^{PDG})^2} + \frac{E_{j1}(1 - \alpha_{E_{j1}})}{\sigma_1^2} + \frac{E_{j2}(1 - \alpha_{E_{j2}})}{\sigma_2^2} \quad (1)$$

The first term is the kinematic constraint of the light jet pair invariant mass to the true mass and width of the  $W$  boson [16].  $\sigma_{1,2}$ , the light jet energy resolutions, are estimated from a Gaussian fit of the difference between the light jet energy and the corresponding quark energy and they are a function of the jet energy.

For each event, pairs of light jets are preselected within a mass window of 30 GeV around the peak value (82 GeV) of the dijet mass distribution that was built considering only events with exactly two light jets (left plot in figure 3). For each preselected light jet pair, this minimization provides the energy scale factors  $\alpha_{E_{j1}}$  and  $\alpha_{E_{j2}}$  and the pair with minimum  $\chi^2$  is assumed to come from the decay  $W(\rightarrow qq')$ . This procedure represents itself an in-situ determination of the light jet energy scale using the sample of hadronic  $W$  boson decay candidates and has the advantage of avoiding miscalibrations in the jet energy scale. Finally, the reconstruction of the hadronic top quark decay chain  $t \rightarrow bW(\rightarrow qq')$  is done by combining the reconstructed hadronic  $W$  boson candidate with the nearest b-jet, providing the three-jet mass distribution  $M_{jjb}$  that will be used to measure the top quark mass (right plot in figure 3).

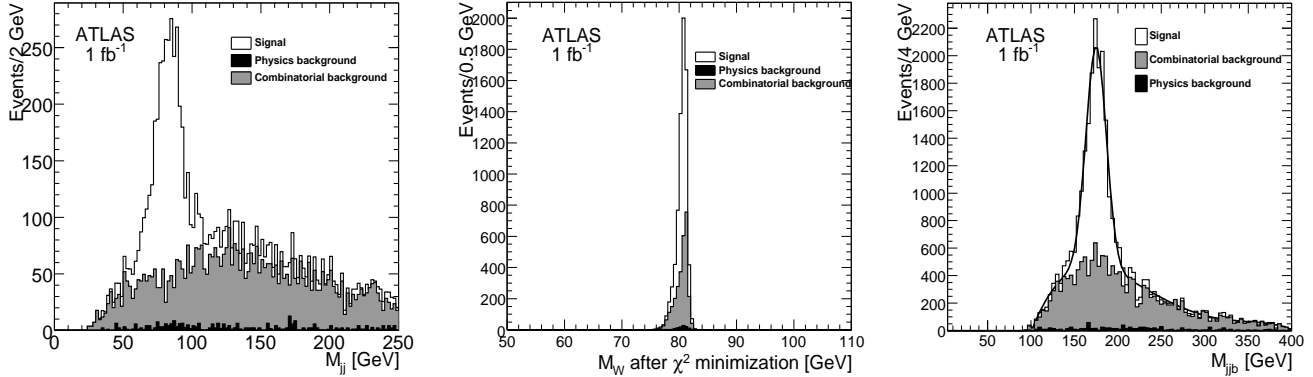


**Figure 3.** Left: invariant mass of light jets for events with only two light jets preselected. Center:  $W$  boson mass after  $\chi^2$  minimization. Right: reconstructed top quark mass with the  $\chi^2$  method, the result of the fit to a Gaussian and a third order polynomial is  $M_{top} = 175.0 \pm 0.2$  GeV and  $\sigma_{M_{top}} = 11.6 \pm 0.2$  GeV using  $t\bar{t}$  MC generated with  $M_{top} = 175$  GeV.

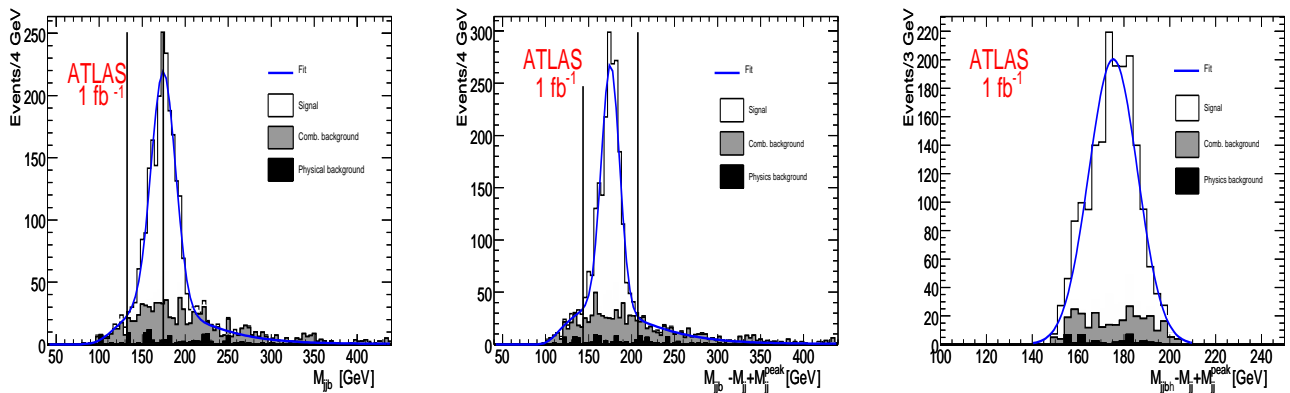


**Figure 4.** Left:  $M_{jjb}$  distribution of hadronically decaying top quark candidates  $t \rightarrow bW(\rightarrow qq')$  obtained with the geometric method. Central: idem after event-by-event subtraction of the offset  $M_{jj} + M_{jj}^{peak}$ . Right: idem after cuts C1, C2, C3 and C4.

In the second method, called the geometric method, the reconstruction of the decay  $W(\rightarrow qq')$  is done by choosing the light pair with the smallest angular distance. The dijet mass of this pair is used to build the  $W$  boson mass distribution  $M_W^{rec}$ . Only those events satisfying  $|M_W^{rec} - M_W^{peak}| < 2\sigma_{M_W}$  with  $\sigma_{M_W} = 10.4$  GeV are kept. At this point, the  $M_{jjb}$  distribution is obtained as in the previous method by assigning the b-jet closest to the hadronic  $W$  boson candidate (see left plot in figure 4). Furthermore, in order to remove at first order the contribution of the light jet energy calibration to the top quark mass resolution, the subtraction of the offset  $M_{jj} + M_{jj}^{peak}$  is performed event-by-event (see central plot in figure 4).

In contrast to the Tevatron philosophy of preserving as much  $t\bar{t}$  signal as possible to minimize the statistical uncertainty, the high production rate of top pairs at the LHC allows stringent selection requirements to reduce the  $t\bar{t}$  combinatorial background and related systematics. For  $t\bar{t}$  combinatorial background rejection the next cuts are proposed for both methods: C1:

$M(W_{had}, b_{lep}) > 200$  GeV, C2:  $M(lepton, b_{lep}) < 160$  GeV, C3:  $|X_1 - \mu_1| < 1.5\sigma_1$  and C4:  $|X_2 - \mu_2| < 2\sigma_2$ .<sup>1</sup> The rejection of the  $t\bar{t}$  combinatorial background can be clearly seen in figure 4 right.

The current measurement of the top quark mass:  $M_{top} = 172.4 \pm 0.7(\text{stat.}) \pm 1.0(\text{syst.})$  GeV [1], has a total error of 1.2 GeV and a relative precision of 0.7%. This precise measurement helps in the constraint of the mass of the Higgs boson. The last electroweak precision tests of the Standard Model incorporate such measurement and indicate that if the Standard Model Higgs boson exists and taking into account the lower limit of 114 GeV from direct searches at LEP2, then its mass will be lower than 185 GeV [17]. With the first  $1 \text{ fb}^{-1}$ , the two experimental methods described in this section achieve a precision of 1 to 3.5 GeV in  $M_{top}$  assuming that the jet energy scale uncertainty is well under control within the range of 1 to 5 %. A precise control of the jet energy scale will therefore be required for ATLAS to contribute significantly in this area, and further to constrain the mass of the Higgs boson.

## 5. Prospects for top quark physics beyond the Standard Model

### 5.1. Measurement of the $W$ boson polarization and sensitivity to anomalous couplings in the $Wtb$ vertex

In the leptonic top quark decay chain  $t \rightarrow W(\rightarrow \ell\nu_\ell)b$ , the measurements of the helicity fractions of  $W$  bosons that are longitudinally polarized  $F_0$ , and with “left-handed” (“right-handed”) polarization  $F_-$  ( $F_+$ ), are sensitive to possible new anomalous couplings:  $V_R$ ,  $V_L$ ,  $g_R$  and  $g_R$  contributing to the  $Wtb$  vertex [18]. In the Standard Model:  $V_L \equiv V_{tb} \approx 0.999$ ,  $V_R = g_R = g_R = 0$  and at leading order,  $F_0 = 0.7$ ,  $F_- = 0.3$  and  $F_+ = 0$  [19].

The analysis techniques developed by ATLAS use the semi-leptonic and di-leptonic  $t\bar{t}$  sample and reconstruct the angular distribution  $\cos(\theta^*)$ , where  $\theta^*$  is the angle between the lepton and the top quark both in the  $W$  boson reference frame, in the top quark decay chain  $t \rightarrow W(\rightarrow \ell\nu_\ell)b$ . From this observable, the helicity fractions can be inferred (see equation 2).

$$\frac{1}{N} \frac{dN}{dcos\theta^*} = \frac{3}{2} \left[ F_0 \left( \frac{\sin\theta^*}{\sqrt{2}} \right)^2 + F_- \left( \frac{1 - \cos\theta^*}{2} \right)^2 + F_+ \left( \frac{1 + \cos\theta^*}{2} \right)^2 \right] \quad (2)$$

The most precise results from the Tevatron (see table 4) are highly statistically limited, with a relative precision of 17% in  $F_0$  and a precision of 0.08-0.1 in absolute numbers for  $F_+$ . With  $1 \text{ fb}^{-1}$  of ATLAS data, the precision will improve to 5% in  $F_0$  and 0.03 in  $F_+$ , with analysis techniques inspired by Tevatron methods [20, 21] in order to extract the helicity fractions from the measured  $\cos\theta^*$  distribution.

**Table 4.** Model independent measurements of the  $W$  boson helicity in top quark decays from the Tevatron versus the ATLAS prospects on the same subject.

Experiment and $\mathcal{L}$	$F_0$	$F_+$
DØ, $1 \text{ fb}^{-1}$ [21]	$0.425 \pm 0.166 \text{ (stat)} \pm 0.102 \text{ (syst)}$	$0.119 \pm 0.090 \text{ (stat)} \pm 0.053 \text{ (syst)}$
CDF, $1.9 \text{ fb}^{-1}$ [20]	$0.66 \pm 0.16 \text{ (stat)} \pm 0.05 \text{ (syst)}$	$-0.3 \pm 0.06 \text{ (stat)} \pm 0.03 \text{ (syst)}$
ATLAS, $1 \text{ fb}^{-1}$ [12]	$0.70 \pm 0.04 \text{ (stat)} \pm 0.03 \text{ (syst)}$	$0.01 \pm 0.02 \text{ (stat)} \pm 0.02 \text{ (syst)}$

<sup>1</sup>  $\mu_{1,2}$  and  $\sigma_{1,2}$  are the mean and width of the experimental distribution of the variables  $X_1 = E_W^* - E_b^* = E_{j1}^* - E_{j2}^* - E_b^* = \frac{M_W^2 - M_b^2}{M_{top}}$  and  $X_2 = 2E_b^* = \frac{M_{top}^2 - M_W^2 - M_b^2}{M_{top}}$ .  $E^*$  stands for the particle energy in the top quark rest frame.

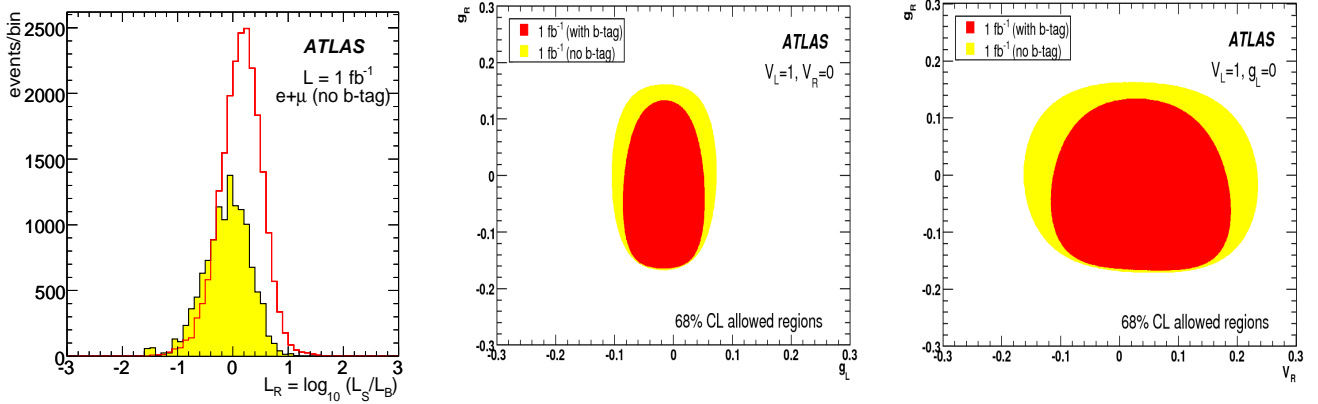


**Figure 5.** Left: Discriminant variable  $L_R$  for  $t\bar{t}$  signal (in solid line) and Standard Model background (shaded region) normalized to  $\mathcal{L} = 1 \text{ fb}^{-1}$ . Central and Right: 68% C.L contours on the  $Wtb$  anomalous couplings for  $\mathcal{L} = 1 \text{ fb}^{-1}$  obtained with the program TopFit [22].

An interesting experimental feature is the  $t\bar{t}$  event reconstruction in the semi-leptonic topology. After a first preselection, with common criteria of the semi-leptonic event selection from the cross section analysis (see section 2.1), the full event reconstruction is done with a minimization technique of a  $\chi^2$  function in which no b-tagging requirement have been used so far:

$$\chi^2 = \frac{(M_{\ell\nu ja} - M_{top})^2}{\sigma_{top}^2} + \frac{(M_{jb_{cjd}} - M_{top})^2}{\sigma_{top}^2} + \frac{(M_{\ell\nu} - M_W)^2}{\sigma_W^2} + \frac{(M_{jc_{jd}} - M_W)^2}{\sigma_W^2}, \quad (3)$$

where  $M_{top} = 175 \text{ GeV}$ ,  $M_W = 80.4 \text{ GeV}$ ,  $\sigma_{top} = 14 \text{ GeV}$  and  $\sigma_W = 10 \text{ GeV}$  are the expected top quark and  $W$  boson mass resolutions and  $\ell$  is the triggering electron or muon. All the possible combinations of the four highest  $p_T$  jets:  $j_{a,b,c,d}$  are considered. After the  $\chi^2$  minimization, the jets assigned to the hadronic  $W$ -boson decay  $j_{c,d}$  are non-b jets and the remaining  $j_{a,b}$  are the b-jets. The preselection is completed by requiring  $\chi^2 < 16$ .

Then, a discriminating variable is built from the ratio of signal and background likelihood functions:  $\mathcal{L}_R = \log_{10}(\mathcal{L}_S/\mathcal{L}_B)$ . Signal and background likelihoods  $\mathcal{L}_{S/B} = \prod_{i=1}^n \mathcal{P}_i^{S/B}$ , are built with eight probability density functions: cosine of the angle of the leptonic top quark  $t \rightarrow W(-\ell\nu_\ell)b$  and the leptonic b-jet, the transverse momentum of the hadronic  $W$ , hadronic and leptonic top quark masses,  $p_T$  of the two b-jets,  $p_T$  of the lepton and  $\sqrt{\chi^2}$  distribution. Finally, the event selection requires  $\mathcal{L}_R > 0.1$  (see left plot in figure 5). With a mature detector and usable b-tagging algorithms, two b-tagged jets at the preselection level can be required and considered accordingly in the  $\chi^2$  function. Moreover, the b-tagging weights can be used themselves as probability density functions to build the discriminant ratio  $\mathcal{L}_R$ .

The ATLAS collaboration has also investigated more sensitive variables to new anomalous couplings, the helicity ratios  $\rho_{R,L} \equiv F_{R,L}/F_0$  and simpler variables to extract information about the  $W$  boson helicity fractions, the asymmetries of events above and below certain values of  $z = \cos\theta^*$ :  $A(z = 0) = A_{FB} = \frac{3}{4}[F_R + F_L]$ ,  $A_-(z = +(2^{2/3} - 1)) = 3\beta[F_0 + (1 + \beta)F_R]$  and  $A_+(z = -(2^{2/3} - 1)) = -3\beta[F_0 + (1 + \beta)F_R]$ , with  $\beta = 2^{1/3} - 1$ . The parametric dependence of the observables  $\rho_L, \rho_R, A_{FB}, A_+$  and  $A_-$  on the top quark anomalous couplings  $V_R, g_L$  and  $g_R$  and their correlations, are used to set bounds to these couplings using the program TopFit [22]. For  $\mathcal{L} = 1 \text{ fb}^{-1}$ , the precision obtained is:  $\Delta V_R/V_R \approx 0.15$ ,  $\Delta g_L/g_L \approx 0.07$  and  $\Delta g_R/g_R \approx 0.15$  (see central and right plots of figure 5 for 68% C.L. contours).

### 5.2. Rare top quark decays

In the Standard Model, the top quark decays via flavor changing neutral currents (FCNC) are highly suppressed by the GIM mechanism and CKM suppression. Beyond the Standard Model scenarios, for instance SUSY models and Two Higgs Doublets models, enhance top quark FCNC decays providing observable branching fractions [23]. The search for rare top quark decays will be performed in the semi-leptonic  $t\bar{t}$  sample, replacing the Standard Model top quark decay  $t \rightarrow bW(\rightarrow q\bar{q}')$  by a rare decay via FCNC ( $t \rightarrow qX, X = \gamma, Z, g$ ). Each of the three decays defines a channel with a different final state topology and with their own event selection, described in table 5. After the event selection, a probabilistic likelihood-based analysis similar to the one described in the previous section 5.1 follows, replacing  $M_{jb,jc,jd}$  in equation 3 by  $M_t^{FCNC} \equiv M_{bq\gamma}, M_{bqg}$  and  $M_{bZq}$  respectively and using new variables for the probability density functions used to build the signal and background likelihoods. No cut on the discriminant variable  $L_R$  is applied (see left plot in figure 6 for the distribution of  $L_R$  in  $t\bar{t} \rightarrow bW(\rightarrow \ell\nu_\ell)q\gamma$  events.

**Table 5.** Event selection, expected number of background events in  $\mathcal{L} = 1 \text{ fb}^{-1}$ , signal efficiencies and variables used as probability density functions to build the signal and background likelihood discriminating functions.

Channel	$t\bar{t} \rightarrow bWq\gamma$	$t\bar{t} \rightarrow bWqg$	$t\bar{t} \rightarrow bWqZ$
Event Selection	$= 1\ell(p_T > 25 \text{ GeV})$ $\geq 2j(p_T > 20 \text{ GeV})$ $= 1\gamma(p_T > 75 \text{ GeV})$ $E_T^{miss} > 20 \text{ GeV}$	$= 1\ell(p_T > 25 \text{ GeV})$ $= 3j(p_T > 40, 20, 20 \text{ GeV})$ $= 0\gamma(p_T > 15 \text{ GeV})$ $E_T^{miss} > 20 \text{ GeV}$ $E_{vis} > 300 \text{ GeV}$ $p_{Tg} > 75 \text{ GeV}$ $125 < m_{qg} < 200 \text{ GeV}$	$= 3\ell(p_T > 25, 15, 15 \text{ GeV})$ $\geq 2j(p_T > 30, 20 \text{ GeV})$ $= 0\gamma(p_T > 15 \text{ GeV})$ $E_T^{miss} > 20 \text{ GeV}$ $2 \ell \text{ same flavour}$ $\text{oppositely charged}$
$N_{bkg}$	$650 \pm 60$	$19300 \pm 40$	$1300 \pm 60$
Efficiency %	$7.6 \pm 0.2$	$2.9 \pm 0.1$	$7.6 \pm 0.2$
PDF variables for $L_R$	$M_t^{FCNC} \equiv M_{bq\gamma}$ $M_{b\gamma}, p_T^\gamma$	$M_t^{FCNC} \equiv M_{bqg}$ $M_t^{SM} \equiv M_{\ell\nu j}$ $M_{qb}, p_T^b, p_T^q, \alpha_{\ell g}$	$M_t^{FCNC} \equiv M_{bZq}$ $M_{\ell\ell}^{min}, m_{bZ}$ $m_{qb}, p_T^{\ell_3}, p_T^q$

In the absence of a FCNC top quark decay signal, the expected 95% C.L. limits for an integrated luminosity of  $\mathcal{L} = 1 \text{ fb}^{-1}$  are:  $\text{BR}(t \rightarrow q\gamma) < 10^{-3}$ ,  $\text{BR}(t \rightarrow Zq) < 10^{-3}$  and  $\text{BR}(t \rightarrow qg) < 10^{-2}$ . The uncertainties in these 95% C.L. limits due to systematic errors are 32%, 25% and 27% respectively.

### 5.3. Resonant top pair production

The ATLAS collaboration has developed a model independent search for resonances  $Z' \rightarrow t\bar{t}$ . The basic idea is to look for deviations in the  $t\bar{t}$  invariant mass spectrum  $d\sigma/dM_{t\bar{t}}$  of the semi-leptonic  $t\bar{t}$  sample. At  $M_{Z'} > 1000 \text{ GeV}$ , boosted top quarks decaying hadronically produce collimated jets. Consequently, the efficiency of the standard  $t\bar{t}$  reconstruction techniques used for high precision measurements of the top quark mass decreases from 5% at  $M_{Z'} = 700 \text{ GeV}$  down to less than 1% for  $M_{Z'} > 1500 \text{ GeV}$ . Then, innovative techniques to reconstruct the hadronic top “monojets” at high  $p_T$  are currently under strong development [24]. They are aiming at the discrimination of top monojet from QCD jets with heavy flavour. They make use of offline b-tagging algorithms optimized for jets at high  $p_T$  and they give sensitivity to the inner structure of the monojet using customized jet clustering algorithms.

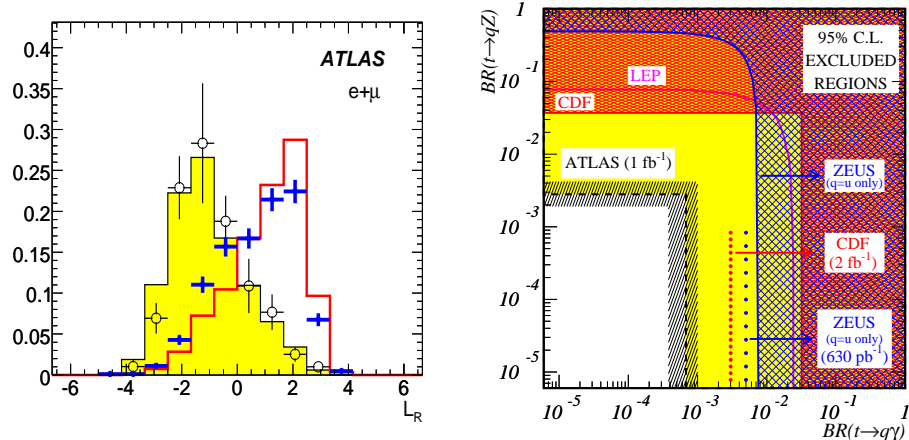


**Figure 6.** Left:  $L_R$  normalized distribution for  $t\bar{t} \rightarrow bWq\gamma$  events: background in shaded region versus signal. Right: 95% C.L. observed limits in the two dimensional plane of  $BR(t \rightarrow Zq)$  versus  $BR(t \rightarrow q\gamma)$  for LEP, ZEUS and CDF collaborations in comparison with the expected limits at ZEUS (630  $\text{pb}^{-1}$ ), CDF (2  $\text{fb}^{-1}$ ) (dotted lines) and ATLAS (1  $\text{fb}^{-1}$ ) with 1 $\sigma$  systematic band (dashed line and band).

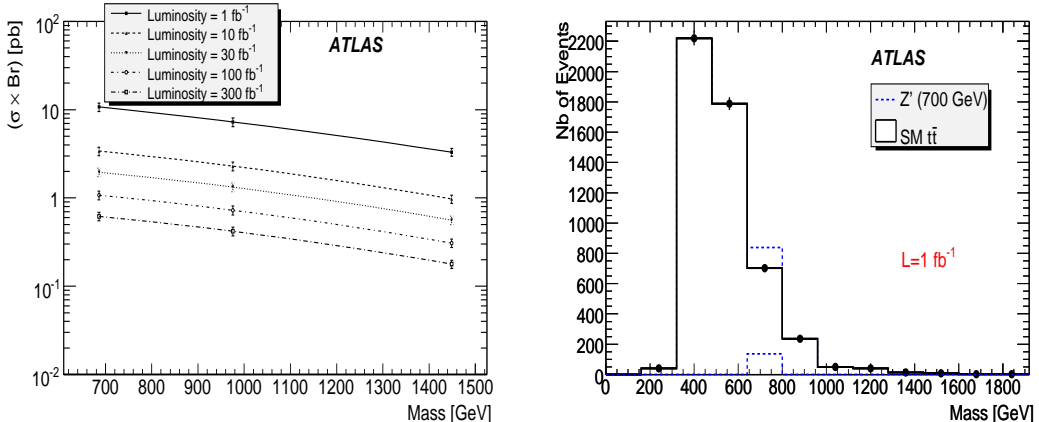


**Figure 7.** Left:  $5\sigma$  discovery potential of a generic narrow resonance  $Z' \rightarrow t\bar{t}$  as a function of its mass and the integrated luminosity. Right: Expected  $t\bar{t}$  invariant mass spectrum  $d\sigma/dM_{t\bar{t}}$  with  $L = 1 \text{ fb}^{-1}$  and a resonance with mass  $M_{Z'} = 700 \text{ GeV}$  produced with  $\sigma \times Br(Z' \rightarrow t\bar{t}) = 11 \text{ pb}$ .

The Tevatron experiments have set up limits to narrow resonances in a specific model: in a Topcolor assisted technicolor model, the production of a narrow ( $\Gamma_{Z'} = 0.012 M_{Z'}$ ) and leptophobic  $Z'$  decaying to  $t\bar{t}$  is excluded at 95% CL with  $M_{Z'} < 700 \text{ GeV}$  [25]. The  $5\sigma$  discovery potential of the ATLAS detector has been evaluated counting  $t\bar{t}$  events over the invariant mass spectrum  $700 < M_{Z'} < 1500 \text{ GeV}$  in a sliding mass window that has a width twice the detector resolution for certain resonance mass (see left plot in figure 7). In the first  $1 \text{ fb}^{-1}$ , a resonance with  $M_{Z'} = 700 \text{ GeV}$  would be discovered with  $5\sigma$  significance if it was produced with  $\sigma \times Br(Z' \rightarrow t\bar{t}) > 11 \text{ pb}$ .

## 6. Conclusions

Top quark physics will play an important role in the early days of the data taking of the ATLAS experiment at the LHC. With only  $\mathcal{L} = 100 \text{ pb}^{-1}$ ,  $\sigma(pp \rightarrow t\bar{t})$  can be measured with an uncertainty of 5-10 % dominated by systematics, excluding the luminosity uncertainty. ATLAS will get this early data probably at  $\sqrt{s} = 10 \text{ TeV}$  at the center-of-mass energy or perhaps even lower: prospects summarized in these proceedings are currently being reevaluated.

With the first  $\mathcal{L} = 1 \text{ fb}^{-1}$ , the t-channel  $pp \rightarrow tqb + X$  is the most promising one for an early observation of single top quark production at the LHC. If the Jet Energy Scale uncertainty is controlled within a range 1-5%, then a precision of 1-3 GeV should be achievable in the measurement of  $M_{top}$ . The study of top quark properties, for example, the polarization of the  $W$  boson in the top quark decay chain  $t \rightarrow W(\rightarrow \ell\nu_b)$  as well as deviations in the  $t\bar{t}$  invariant mass spectrum  $d\sigma/dM_{t\bar{t}}$  may provide a hint of physics beyond the Standard Model.

## Acknowledgments

S.C. is indebted to all the colleagues, funding agencies, CERN and Institutions that have contributed to the amazing effort of the construction and the installation of the LHC proton proton collider and the ATLAS detector. The work of S.C. has been funded by a project of the Spanish Ministry of Science and Innovation (MICINN): PORT2008-01, by a project of the Generalitat Valenciana (GV): GVPRE/2008/062, and by a Ramón y Cajal contract funded by both the MICINN and the Spanish Research Council (CSIC).

## References

- [1] The Tevatron Electroweak Working Group, for the CDF and DØ Collaborations, arXiv:0808.1089v1. [http://www-cdf.fnal.gov/physics/new/top/2008/mass/tevcombination\\_july/](http://www-cdf.fnal.gov/physics/new/top/2008/mass/tevcombination_july/)
- [2] [http://www-cdf.fnal.gov/physics/new/top/2008/xsection/ttbar\\_combined\\_3invfb/](http://www-cdf.fnal.gov/physics/new/top/2008/xsection/ttbar_combined_3invfb/)
- [3] <http://www-cdf.fnal.gov/physics/new/top/top.html>
- [4] [http://www-d0.fnal.gov/Run2Physics/top/top\public\\\_web\\\_\\\_pages/top\\_public.html](http://www-d0.fnal.gov/Run2Physics/top/top\public\_web\_\_pages/top_public.html)
- [5] R. Bonciani, S. Catani, M. Mangano, P. Nason, Nucl.Phys.B529:424-450(1998).
- [6] M. Cacciari, S. Frixione, G. Ridolfi, M. Mangano and P. Nason, arXiv:0804(2800).
- [7] N. Kidonakis and R. Vogt, arXiv:0805:3844(2008).
- [8] S. Moch and P. Uwer, arXiv:0807.2794(2008).
- [9] <http://press.web.cern.ch/Press/PressReleases/Releases2008/PR08.08E.html>
- [10] <http://press.web.cern.ch/Press/PressReleases/Releases2008/PR14.08E.html>
- [11] <http://press.web.cern.ch/press/PressReleases/Releases2009/PR02.09E.html>
- [12] G. Aad *et al.* ATLAS Collaboration, *Expected Performance of the ATLAS Experiment: Detector, Trigger and Physics*. CERN-OPEN 2008-020, [arXiv:0901.0512].
- [13] The DØ Collaboration (V.M. Abazov *et al.*). Phys.Rev.Lett.98:181802(2007).
- [14] [http://www-cdf.fnal.gov/physics/new/top/public\\_singletop.html](http://www-cdf.fnal.gov/physics/new/top/public_singletop.html) The CDF Collaboration (T. Aaltonen *et al.* ). arXiv:0809.2581.
- [15] J. Parsons, *see these proceedings*
- [16] <http://pdg.lbl.gov/>
- [17] The LEP Electroweak Working Group. <http://lepewwg.web.cern.ch/LEPEWWG/>
- [18] F. del Águila and J.A. Aguilar-Saavedra. Phys.Rev.D67:014009(2003).
- [19] G. L. Kane, G.A. Ladinsky and C.P. Yuan, Phys.Rev.D45:124-141(1992).
- [20] The CDF Collaboration (T. Aaltonen *et al.*). Submitted to Phys.Lett.B e-Print: arXiv:0811.0344
- [21] The DØ Collaboration (V.M. Abazov *et al.*). Phys.Rev.Lett.100:062004,2008. e-Print: arXiv:0711.0032
- [22] J.A. Aguilar-Saavedra, J. Carvalho, N. Castro, A. Onofre and F. Veloso, Eur. Phys. J.C 50 (2007) 519.
- [23] J.A. Aguilar-Saavedra. Acta Phys.Polon.B35:2695-2710(2004). e-Print: hep-ph/0409342
- [24] G. Brooijmans, “High  $p_T$  hadronic top quark identification. Part I: Jet mass and Ysplitter.” ATL-PHYS-CONF-2008-008. M. Vos, “High  $p_T$  hadronic top quark identification: Part II: The lifetime signature”. ATL-PHYS-CONF-2008-016.
- [25] The DØ Collaboration (V.M. Abazov *et al.*). Phys.Lett.B668:98-104,2008. e-Print: arXiv:0804.3664; the CDF Collaboration (T. Aaltonen *et al.*). Phys.Rev.D77:051102,2008. e-Print: arXiv:0710.5335